REVISITING THE ROLE OF LANGUAGE PRIORS IN VISION-LANGUAGE MODELS

Anonymous authors
Paper under double-blind review

ABSTRACT

Vision-language models (VLMs) are impactful in part because they can be applied to a variety of visual understanding tasks in a zero-shot fashion, without any fine-tuning. We study currently popular *generative VLMs* that are trained for next-word generation given the image. We explore their zero-shot performance on the illustrative task of image-text retrieval across 8 popular vision-language benchmarks. Our first observation is that they can be repurposed for discriminative tasks (such as image-text retrieval) by simply computing the match score of generating a particular text string given an image. We call this probabilistic score the *Visual Generative Pre-Training Score* (VisualGPTScore). While the VisualGPTScore produces near-perfect accuracy on some retrieval benchmarks, it produces poor accuracy on others. We analyze this behavior through a probabilistic lens, pointing out that some benchmarks inadvertently capture unnatural language distributions by creating adversarial but unlikely text captions. In fact, we demonstrate that even a "blind" language model that ignores any image evidence can sometimes outperform all prior art, reminiscent of similar challenges faced by the visual-question answering (VQA) community many years ago. We derive a probabilistic post-processing scheme that controls for the amount of linguistic bias in generative VLMs at test time without having to retrain or fine-tune the model. We show that the VisualGPTScore, when appropriately debiased, is a strong zero-shot baseline for vision-language understanding, oftentimes producing state-of-the-art accuracy.

1 INTRODUCTION

Vision-language models (VLMs) trained on web-scale datasets will likely serve as the foundation for next-generation visual understanding systems. One reason for their widespread adoption is their ability to be used in an "off-the-shelf" (OTS) or zero-shot manner, without fine-tuning on any target application of interest. We study their OTS use on the task of image-text retrieval (e.g., given an image, predict which of K possible captions is true) across a suite of 8 popular benchmarks.

Challenges. While the performance of foundational VLMs is impressive, many open challenges remain. Recent analysis (Kamath et al., 2023; Yuksekgonul et al., 2022) points out that leading VLMs such as CLIP (Radford et al., 2021) may often degrade to "bag-of-words" that confuse captions such as `"the horse is eating the grass"` and `"the grass is eating the horse"`. This makes it difficult to use VLMs to capture *compositions* of objects, attributes, and their relations. But somewhat interestingly, large-scale language models (LLMs) trained for autoregressive next-token prediction (Brown et al., 2020) seem to be able to capture such distinctions, which we investigate below. A related but under-appreciated difficulty is that of *benchmarking* the performance of visio-linguistic reasoning. Perhaps the most well-known example in the community is that of the influential VQA benchmarks (Antol et al., 2015), which could be largely solved by exploiting linguistic biases in the dataset – concretely, questions about images could often be answered by "blind" language-only models that did not look at the image (Goyal et al., 2017). Notably, we find that such blind algorithms can still produce strong performance on many contemporary image-text retrieval benchmarks where VLMs may struggle.

Generative models for discriminative tasks. We tackle the above challenges by revisiting the role of language priors through a probabilistic lens. To allow for a probabilistic treatment, we focus on generative VLMs that take an image as input and stochastically generate text via next-token

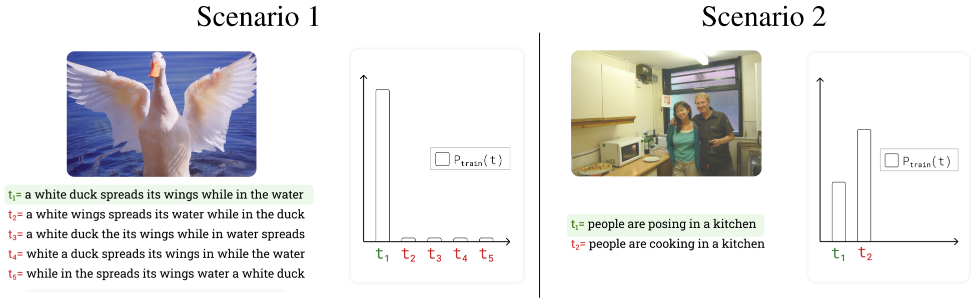
Scenario 1
t_1= a white duck spreads its wings while in the water
t_2= a white wings spreads its water while in the duck
t_3= a white duck the its wings while in water spreads
t_4= white a duck spreads its wings in while the water
t_5= while in the spreads its wings water a white duck
$P_{train}(t)$
t_1 t_2 t_3 t_4 t_5
Scenario 2
t_1= people are posing in a kitchen
t_2= people are cooking in a kitchen
$P_{train}(t)$
t_1 t_2

Figure 1: **Two train-test shifts encountered in image-to-text retrieval tasks.** Scenario 1 constructs negative text captions by shuffling words in the true caption (as in ARO-Flickr), but this produces implausible text such as `white a duck spreads its wings in while the water`. Here, exploiting the language bias of the training set will help since it will downweight the match score for negative captions. In fact, a blind language-only model can easily identify the correct caption. Scenario 2 constructs alternative text captions that are curated to be plausible (as in SugarCrepe). Here, the language bias of the training set may hurt, since it will prefer to match common captions (that score well under the language prior) as shown on the right.

prediction (Li et al., 2022; 2023). We first demonstrate that such models can be easily repurposed for discriminative tasks (such as retrieval) by setting the match score for an image-text pair to be the probability that the VLM would generate that text from the given image. We call this probability score the Visual Generative Pre-Training Score, or VisualGPTScore. Computing the VisualGPTScore is even more efficient than next-token generation since given an image, all tokens from a candidate text string can be evaluated in parallel. Though conceptually straightforward, such an approach (to our knowledge) has not been proposed in the literature. In fact, the generative VLMs that we analyze train *separate* discriminative heads for matching/classifying image-text pairs (Li et al., 2022), but we find that their language generation head itself produces better scores for matching (since it appears to better capture compositions). Indeed, OTS VisualGPTScore by itself performs surprisingly well on many benchmarks, even producing near-perfect accuracy on ARO (Yuksekgonul et al., 2022). But it still struggles on other benchmarks such as Winoground (Thrush et al., 2022). We analyze this below.

The role of language priors. We analyze the discrepancy in performance across benchmarks from a probabilistic perspective. Our key insight is that many benchmark biases can be formalized as mismatching distributions over text between train and test data - $P_{train}(\text{text})$ versus $P_{test}(\text{text})$. We use a first-principles analysis to account for distribution shift by simply reweighting the VisualGPTScore with the Bayes factor $P_{test}(\text{text})/P_{train}(\text{text})$, a process we call *debiasing*. To compute the Bayes reweighting factor, we need access to both the train and test language prior. We compute $P_{train}(\text{text})$ from an OTS VLM with Monte-Carlo samples of $P_{train}(\text{text}|\text{image})$ computed on trainset or Gaussian noise images. Because $P_{test}(\text{text})$ may require access to the test set, we explore simplifying assumptions that assume it is (a) identical to $P_{train}(\text{text})$, (b) uninformative/uniform, or (c) tunable from a held-out val set. Our analysis helps explain the strong performance of the VisualGPTScore on certain benchmarks and its poor performance on others. Furthermore, this analysis provides simple strategies for improving performance with debiasing. We finally show a theoretical connection between debiasing and mutual information, which can be seen as a method for removing the effect of marginal priors when computing joint probability scores.

Empirical Analysis. We present an exhaustive empirical analysis of the OTS VisualGPTScore (and its debiased variants) for open-sourced image-conditioned language models (Li et al., 2022; 2023) across 8 popular vision-language benchmarks. We first point out that VisualGPTScore by itself produces SOTA accuracy on certain benchmarks like ARO (Yuksekgonul et al., 2022) where its inherent language bias helps remove incorrect text caption candidates that are also unnatural (such as ``a white duck the its wings while in water" as shown in Fig. 1). In fact, we show that blind baselines also do quite well on such benchmarks, since language-only models can easily identify such poor captions. However, such language biases do not work well on benchmarks where incorrect caption candidates are also realistic. Here, VisualGPTScore should be debiased so as not to naively prefer more common captions that score well under its language prior. When given access to a val set that reveals the amount of language bias in the benchmark, debiasing consistently improves performance on benchmarks such as Flickr30K (Young et al., 2014) and Winoground (Thrush et al., 2022). Interestingly, we find that debiasing can also improve accuracy on the *train* set used to learn the generative VLM, indicating that such models learn biased estimates of the true conditional distribution $P_{train}(\text{text}|\text{image})$. We describe this further in our appendix.

2 Related Works

Vision-language modelling. State-of-the-art VLMs like CLIP (Radford et al., 2021) are pre-trained on web-scale image-text datasets (Schuhmann et al., 2021; 2022) using discriminative objectives including image-text contrastive (ITC) (Radford et al., 2021; Jia et al., 2021) and image-text matching (ITM) (Li et al., 2021; 2022) loss, typically formulated as $P(\text{match}|\text{image}, \text{text})$. These pre-trained models exhibit robust zero-shot and few-shot (Lin et al., 2023; Wortsman et al., 2022) performance on traditional discriminative tasks (Deng et al., 2009; Lin et al., 2014), often on par with fully-supervised models. More recently, image-conditioned language models like Flamingo (Alayrac et al., 2022) and BLIP (Li et al., 2022; 2023) incorporate generative objectives (Bengio et al., 2003) primarily for downstream tasks such as captioning (Agrawal et al., 2019) and VQA (Goyal et al., 2017).

Visio-linguistic compositionality. Benchmarks like ARO (Yuksekgonul et al., 2022), Crepe (Ma et al., 2022), Winoground (Thrush et al., 2022), EqBen (Wang et al., 2023), VL-CheckList (Zhao et al., 2022), and SugarCrepe (Hsieh et al., 2023) show that discriminative scores of VLMs, such as ITCScore and ITMScore, fail on their image-text retrieval tasks that assess compositional reasoning. Concurrently, advances on these tasks often involve fine-tuning discriminative VLMs with more data. One of the most popular approaches, NegCLIP (Yuksekgonul et al., 2022), augments CLIP using programmatically generated negatives from original texts. Extending this, subsequent studies propose more expensive and heavily-engineered solutions. SyViC (Cascante-Bonilla et al., 2023) fine-tunes VLMs on million-scale synthetic images to augment spatial, attributive, and relation understanding. SGVL (Herzig et al., 2023) and Structure-CLIP (Huang et al., 2023) sample negatives using costly scene graph annotations. MosaiCLIP (Singh et al., 2023) and SVLC (Doveh et al., 2022) use linguistic tools such as scene graph parsers and LLMs to design better negative captions. The most recent DAC (Doveh et al., 2023) leverages a combination of foundation models including BLIP2, ChatGPT, and SAM to rewrite and augment image captions.

Generative pre-training and scoring. Vision models trained with *discriminative* objectives often lack incentives to learn structure information (Brendel & Bethge, 2019; Tejankar et al., 2021). Similarly, early LLMs trained with *discriminative* approaches, such as BERT (Devlin et al., 2018) and RoBERTa (Liu et al., 2019), have also been criticized as bag-of-words models insensitive to word order (Bertolini et al., 2022; Hessel & Schofield, 2021; Papadimitriou et al., 2022; Sinha et al., 2021). Conversely, generative pre-trained LLMs (Radford et al., 2019) demonstrate exceptional compositional understanding while pre-trained solely with a next-token prediction (Bengio et al., 2003) loss. Furthermore, generative scores of LLMs (OpenAI, 2023; Chung et al., 2022; Zhang et al., 2022) have flexible usage in downstream tasks, such as text evaluation (Yuan et al., 2021; Fu et al., 2023) and reranking (Keskar et al., 2019).

3 The role of language priors

In this section, we present a simple probabilistic treatment for analyzing the role of language priors in image-conditioned language models (or generative VLMs). Motivated by their strong but inconsistent performance across a variety of image-text retrieval benchmarks, we analyze their behavior when there exists a mismatch between training and test distributions, deriving simple schemes for addressing the mismatch with reweighting. We conclude by exposing a connection to related work on mutual information.

Computing $P(\mathbf{t}|\mathbf{i})$. To begin our probabilistic treatment, we first show that image-conditioned language models (that probabilistically generate text based on an image) can be repurposed for computing a score between a given image $\mathbf{i}$ and text caption $\mathbf{t}$. The likelihood of a text sequence $\mathbf{t} = \{t_1, t_2, \cdots, t_m\}$ conditioned on image $\mathbf{i}$ is naturally factorized as an autoregressive product (Bengio et al., 2003):

$$P(\mathbf{t}|\mathbf{i}) = \prod_{k=1}^{m} P(t_k|t_{<k}, \mathbf{i}) \tag{1}$$

Image-conditioned language models return back m softmax distributions corresponding to the m terms in the above expression. Text generation requires *sequential* token-by-token prediction, since token t_k must be generated before it can be used as an input to generate the softmax distribution over token t_{k+1}. Interestingly, given an image $\mathbf{i}$ and text sequence $\mathbf{t}$, the above probability can be computed in *parallel* because the entire sequence of tokens $\{t_k\}$ are already available as input. We provide a visual illustration in Figure 2-a.

Train-test shifts. Given the image-conditioned model of $P(\mathbf{t}|\mathbf{i})$ above, we now analyze its behavior when applied to test data distributions that differs from the trainset, denoted as P_{test} versus P_{train}. Recall that any joint distribution over images and text can be factored into a product over a language prior and an image likelihood $P(\mathbf{t}, \mathbf{i}) = P(\mathbf{t})P(\mathbf{i}|\mathbf{t})$. Our analysis makes the strong assumption that the image likelihood $P(\mathbf{i}|\mathbf{t})$ is identical across the train and test data, but the language prior $P(\mathbf{t})$ may differ. Intuitively, this assumes that the visual appearance of entities (such as a "white duck") remains consistent across the training and test data, but the frequency of those entities (as manifested in the set of captions $P(\mathbf{t})$) may vary. We can now derive $P_{test}(\mathbf{t}|\mathbf{i})$ via Bayes rule:

$$P_{test}(\mathbf{t}|\mathbf{i}) \propto P(\mathbf{i}|\mathbf{t})P_{test}(\mathbf{t}) \tag{2}$$

$$= P(\mathbf{i}|\mathbf{t})\frac{P_{train}(\mathbf{t})}{P_{train}(\mathbf{t})}P_{test}(\mathbf{t}) \tag{3}$$

$$\propto P_{train}(\mathbf{t}|\mathbf{i})\frac{P_{test}(\mathbf{t})}{P_{train}(\mathbf{t})} \tag{4}$$

The above shows that the generative pre-training score $P_{train}(\mathbf{t}|\mathbf{i})$ need simply be weighted by the *ratio* of the language priors in the testset versus trainset. Intuitively, if a particular text caption appears *more* often in the testset than the trainset, one should *increase* the score reported by the generative model. However, one often does not have access to the text distribution on the testset. For example, real-world deployments and benchmark protocols may not reveal this. In such cases, one can make two practical assumptions; either the language distribution on test is identical to train, or it is uninformative/uniform (see Figure 1):

$$\text{Scenario 1:} \quad P_{test}(\mathbf{t}) = P_{train}(\mathbf{t}) \qquad \Rightarrow \qquad \text{Optimal score is } P_{train}(\mathbf{t}|\mathbf{i}). \tag{5}$$

$$\text{Scenario 2:} \quad P_{test}(\mathbf{t}) \text{ is uniform.} \qquad \Rightarrow \qquad \text{Optimal score is } \frac{P_{train}(\mathbf{t}|\mathbf{i})}{P_{train}(\mathbf{t})}. \tag{6}$$

Tunable α. In reality, a testset might be a mix of both scenarios. To model this, we consider a soft combination where the language prior on the testset is assumed to be a flattened version of the language prior on the trainset, for some temperature parameter $\alpha \in [0, 1]$:

$$P_{test}(\mathbf{t}) \propto P_{train}(\mathbf{t})^{1-\alpha} \quad \Rightarrow \text{Optimal score is } \frac{P_{train}(\mathbf{t}|\mathbf{i})}{P_{train}(\mathbf{t})^{\alpha}} \tag{7}$$

By setting α to 0 or 1, one can obtain the two scenarios described above. Some deployments (or benchmarks) may benefit from tuning α on a val set.

Implications for retrieval benchmarks. We speculate some benchmarks like ARO-Flickr (Yuksekgonul et al., 2022) are close to scenario 1 because they include negative captions that are *implausible*, such as "a white duck the its wings while in water spreads". Such captions will have a low score under the language prior $P_{train}(\mathbf{t})$ and so reporting the raw generative score $P_{train}(\mathbf{t}|\mathbf{i})$ (that keeps its language prior or bias) will improve accuracy. In fact, we show that applying a *blind* language model (that ignores all image evidence) can itself often identify the correct caption. On the other hand, for test datasets with more *realistic* negative captions (scenario 2), it may be useful to remove the language bias of the trainset, since that will prefer to match to common captions (even if they do not necessarily agree with the input image). This appears to be the case for SugarCrepe (Hsieh et al., 2023), which uses LLMs like ChatGPT to ensure that the negative captions are realistic.

Relationship to prior approaches. Our approach to debiasing is reminiscent of mutual information, which can also be seen as a method for removing the effect of marginal priors when computing joint probability scores. In fact, our Appendix A derives that α-debiasing is equivalent to a form of pointwise mutual information (PMI) known as PMI^k for $k = \frac{1}{\alpha}$.

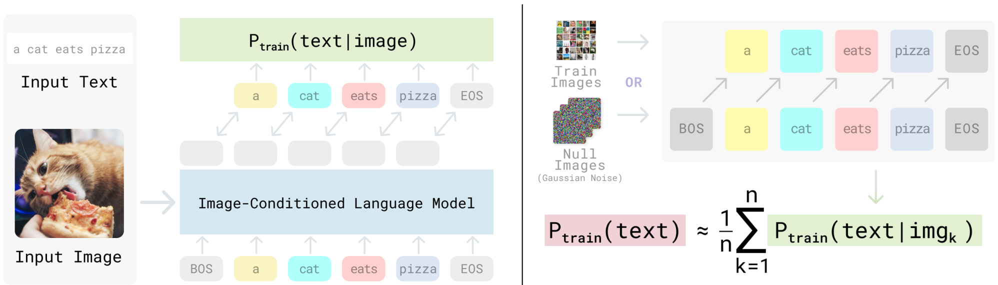

(a) $P_{train}(\mathbf{t}|\mathbf{i})$ through generative VLMs

(b) $P_{train}(\mathbf{t})$ via Monte Carlo sampling

Figure 2: **Estimating $P_{train}(\mathbf{t}|\mathbf{i})$ and $P_{train}(\mathbf{t})$ from generative VLMs.** Figure (a) shows how image-conditioned language models such as Li et al. (2022) that generate text based on an image can be repurposed for computing $P_{train}(\mathbf{t}|\mathbf{i})$, which is factorized as a product of $\prod_{k=1}^{m} P(t_k|t_{<k}, \mathbf{i})$ for a sequence of m tokens. These terms can be efficiently computed in *parallel*, unlike *sequential* token-by-token prediction for text generation. Figure (b) shows two approaches for Monte Carlo sampling of $P_{train}(\mathbf{t})$. While the straightforward approach is to sample trainset images, we find that using as few as three "null" (Gaussian noise) images can achieve more robust estimates.

4 Experimental results on I-to-T retrieval

In this section, we verify our hypothesis on I-to-T retrieval benchmarks using state-of-the-art multimodal generative VLMs. In particular, we adopt image-conditioned language models such as BLIP (Li et al., 2022) as the learned estimator of $P_{train}(\mathbf{t}|\mathbf{i})$. Then, we discuss how we perform Monte Carlo estimation of $P_{train}(\mathbf{t})$, including a novel efficient sampling method based on "content-free" Gaussian noise images. Finally, we show the state-of-the-art results of our generative approach on existing I-to-T retrieval tasks.

Preliminaries. We leverage OTS image-conditioned language models (Yu et al., 2022; Alayrac et al., 2022; Li et al., 2023) to estimate $P_{train}(\mathbf{t})$. For ablation, we use the open-sourced BLIP models (Li et al., 2022), trained on public image-text corpora using discriminative (ITC and ITM) and generative (captioning) objectives. Discriminative objectives typically model $P(\text{match}|\mathbf{t}, \mathbf{i})$. For example, ITCScore calculates cosine similarity scores between image and text features using a dual-encoder; ITMScore jointly embeds image-text pairs via a fusion-encoder and returns softmax scores from a binary classifier. Lastly, we term the generative score as **Visual G**enerative **P**re-**T**raining Score (**VisualGPTScore**). While BLIP is pre-trained using all three objectives, this generative score has not been applied to discriminative tasks before our work.

Implementing VisualGPTScore. Our method calculates an average of the log-likelihoods of t_k at each token position k and applies an exponent to cancel the log:

$$\textbf{VisualGPTScore}(\mathbf{t}, \mathbf{i}) := e^{\frac{1}{m}\sum_{k=1}^{m} \log(P(t_k|t_{<k}, \mathbf{i}))} \tag{8}$$

To condition on an input image, BLIP uses a multimodal casual self-attention mask (Li et al., 2022) in its image-grounded text decoder, i.e., each text token attends to all its preceding vision and text tokens. We emphasize that VisualGPTScore has the same computational cost as ITMScore, which uses the same underlying transformer but with a bi-directional self-attention mask to encode an image-text pair. We address potential biases of this estimator in Appendix C.

Estimating $P_{train}(\mathbf{t})$ using Monte Carlo sampling (oracle approach). Given $P_{train}(\mathbf{t}|\mathbf{i})$, we can estimate $P_{train}(\mathbf{t})$ via classic Monte Carlo sampling (Shapiro, 2003), by drawing n images from the train distribution, such as LAION114M (Schuhmann et al., 2021) for BLIP:

$$P_{train}(\mathbf{t}) \approx \frac{1}{n}\sum_{k=1}^{n} P_{train}(\mathbf{t}|\mathbf{i}_k) \tag{9}$$

Reducing sampling cost with content-free images (our approach). The above Equation 9 requires many trainset samples to achieve robust estimates. To address this, we draw inspiration from (Zhao et al., 2021), which uses a *content-free* text prompt "N/A" to calibrate the probability of a text from LLMs, i.e., $P(\mathbf{t}|\text{"N/A"})$. To apply this to our generative VLMs, we choose to sample "null" inputs

Score	Method	**ARO**			
		Rel	Attr	COCO	Flickr
Random	-	50.0	50.0	20.0	20.0
Text-Only	Vera	61.7	82.6	59.8	63.5
	Grammar	59.6	58.4	74.3	76.3
$P_{LLM}(\mathbf{t})$	BART	81.1	73.6	95.0	95.2
	Flan-T5	84.4	76.5	98.0	98.2
	OPT	84.7	79.8	97.9	98.6
$P_{train}(\mathbf{t})$	BLIP	87.6	80.7	98.6	99.1
$P(\text{match}\|\mathbf{t},\mathbf{i})$	CLIP	59.0	62.0	59.0	46.0
	LAION2B-CLIP	51.6	61.9	25.2	30.2
	LAION5B-CLIP	46.1	57.8	26.1	31.0
	NegCLIP	81.0	71.0	91.0	86.0
	Structure-CLIP	83.5	85.1	-	-
	SyViC	80.8	72.4	92.4	87.2
	SGVL	-	-	87.2	91.0
	MosaiCLIP	82.6	78.0	87.9	86.3
	DAC-LLM	81.3	73.9	94.5	95.7
	DAC-SAM	77.2	70.5	91.2	93.9
	BLIP-ITC	63.1	81.6	34.3	41.7
	BLIP-ITM	58.7	90.3	45.1	51.3
$\frac{P_{train}(\mathbf{t}\|\mathbf{i})}{P_{train}(\mathbf{t})^{\alpha}}$	Ours ($\alpha = 0$)	**89.1**	**95.3**	**99.4**	**99.5**
	Ours ($\alpha = 1$)	68.1	87.9	32.4	44.5
	Ours ($\alpha = \alpha^{*}$)	**89.1**	**95.4**	**99.4**	**99.5**

(a) Accuracy on ARO

Score	Method	**VL-CheckList**		
		Object	Attribute	Relation
Random	-	50.0	50.0	50.0
Text-Only	Vera	82.5	74.0	85.7
	Grammar	58.0	52.4	68.5
$P_{LLM}(\mathbf{t})$	BART	52.0	51.0	45.1
	Flan-T5	60.3	55.0	49.3
	OPT	59.3	48.8	60.0
$P_{train}(\mathbf{t})$	BLIP	68.2	58.7	75.9
$P(\text{match}\|\mathbf{t},\mathbf{i})$	CLIP	81.6	67.6	63.1
	LAION2B-CLIP	84.7	67.8	66.5
	LAION5B-CLIP	87.9	70.3	63.9
	NegCLIP	81.4	72.2	63.5
	SyViC	-	70.4	69.4
	SGVL	85.2	78.2	80.4
	SLVC	85.0	72.0	69.0
	DAC-LLM	87.3	77.3	86.4
	DAC-SAM	88.5	75.8	89.8
	BLIP-ITC	90.6	80.3	73.5
	BLIP-ITM	89.9	80.7	67.7
$\frac{P_{train}(\mathbf{t}\|\mathbf{i})}{P_{train}(\mathbf{t})^{\alpha}}$	Ours ($\alpha = 0$)	92.6	78.7	90.8
	Ours ($\alpha = 1$)	90.4	77.6	77.8
	Ours ($\alpha = \alpha^{*}$)	**94.4**	**82.1**	**92.8**

(b) Accuracy on VL-CheckList

Score	Method	**SugarCrepe**		
		Replace	Swap	Add
Random	-	50.0	50.0	50.0
Text-Only	Vera	49.5	49.3	49.5
	Grammar	50.0	50.0	50.0
$P_{LLM}(\mathbf{t})$	BART	48.4	51.9	61.2
	Flan-T5	51.4	57.6	40.9
	OPT	58.5	66.6	45.8
$P_{train}(\mathbf{t})$	BLIP	75.9	77.1	70.9
$P(\text{match}\|\mathbf{t},\mathbf{i})$	CLIP	80.8	63.3	75.1
	LAION2B-CLIP	86.5	68.6	88.4
	LAION5B-CLIP	85.0	68.0	89.6
	NegCLIP	88.3	76.2	90.2
	BLIP-ITC	85.8	73.8	85.7
	BLIP-ITM	88.7	81.3	87.6
$\frac{P_{train}(\mathbf{t}\|\mathbf{i})}{P_{train}(\mathbf{t})^{\alpha}}$	Ours ($\alpha = 0$)	93.3	91.0	91.0
	Ours ($\alpha = 1$)	83.2	85.5	85.9
	Ours ($\alpha = \alpha^{*}$)	**95.1**	**92.4**	**97.4**

(c) Accuracy on SugarCrepe

Score	Method	**Crepe**		
		Atom	Swap	Negate
Random	-	16.7	16.7	16.7
Text-Only	Vera	43.7	70.8	66.2
	Grammar	18.2	50.9	9.8
$P_{LLM}(\mathbf{t})$	BART	38.8	53.3	44.4
	Flan-T5	43.0	69.5	13.6
	OPT	53.3	72.7	5.0
$P_{train}(\mathbf{t})$	BLIP	55.4	69.7	60.8
$P(\text{match}\|\mathbf{t},\mathbf{i})$	CLIP	22.3	26.6	28.8
	LAION2B-CLIP	23.6	24.8	18.0
	LAION5B-CLIP	24.2	23.9	20.1
	BLIP-ITC	24.8	17.7	26.5
	BLIP-ITM	29.5	20.7	25.5
$\frac{P_{train}(\mathbf{t}\|\mathbf{i})}{P_{train}(\mathbf{t})^{\alpha}}$	Ours ($\alpha = 0$)	**73.2**	**78.1**	**79.6**
	Ours ($\alpha = 1$)	20.6	28.3	35.6
	Ours ($\alpha = \alpha^{*}$)	**73.3**	**78.1**	**79.6**

(d) Accuracy on Crepe

Table 1: **OTS generative VLMs are SOTA on image-to-text retrieval benchmarks.** We begin by evaluating blind language models (in red). Surprisingly, this already produces SOTA accuracy on certain benchmarks such as ARO-Flickr, compared to the best discriminative approaches (in gray). We also find that blind inference of generative VLMs, $P_{train}(\mathbf{t})$ via sampling Gaussian noise images (in blue), often performs better and achieve above-chance performance even on the most recent SugarCrepe. Next, we show that simply repurposing a generative VLM's language generation head for computing image-text scores (VisualGPTScore in yellow), which corresponds to $\alpha = 0$, consistently produces SOTA accuracy across all benchmarks. Finally, debiasing this score by tuning α on val set (in green) further improves performance, establishing the new SOTA.

as Gaussian noise images. As a result, our approach requires as few as three images to compute Eq. 9 by sampling from Gaussian noise images with a mean of 0.4 and a standard deviation of 0.25. We find this method to be less computationally demanding and just as effective as sampling thousands of images from trainset. We provide a visual illustration of this method in Figure 2-b. We include sampling details in Appendix B.

Benchmarks and evaluation protocols. We comprehensively report on four popular I-to-T retrieval benchmarks, including ARO (Yuksekgonul et al., 2022), Crepe (Ma et al., 2022), SugarCrepe Hsieh et al. (2023), and VL-CheckList (Zhao et al., 2022). In these datasets, each image has a single positive caption and multiple negative captions. ARO (Yuksekgonul et al., 2022) has four datasets: VG-Relation, VG-Attribution, COCO-Order, and Flickr30k-Order. SugarCrepe (Hsieh et al., 2023) has three datasets: Replace, Swap, and Add. For Crepe (Ma et al., 2022), we use the entire productivity set and report on three datasets: Atom, Negate, and Swap. VL-CheckList (Zhao et al., 2022) has three datasets: Object, Attribute, and Relation. We visualize all datasets in Appendix Table 13.

SOTA performance on all four benchmarks. In Table 1, we show that our OTS generative approaches, based on the BLIP model pre-trained on LAION-114M with ViT-L image encoder, achieves state-of-the-art results on all benchmarks. We outperform the best discriminative VLMs, including LAION5B-CLIP, and consistently surpass other heavily-engineered solutions, including NegCLIP, SyViC, MosaiCLIP, DAC, SVLC, SGVL, Structure-CLIP, all of which fine-tune CLIP on much more data. Details on how we report the baseline results can be found in Appendix E. For reference, we also include results of text-only Vera and Grammar from Hsieh et al. (2023). To show that even the most recent SugarCrepe is not exempt from language biases, we run two more text-only methods:

1. $P_{LLM}(\mathbf{t})$: passing captions into a pure LLM, such as BART-base (Yuan et al., 2021), FLAN-T5-XL (Chung et al., 2022), and OPT-2.7B (Zhang et al., 2022), to compute a text-only GPTScore (Fu et al., 2023).
2. $P_{train}(\mathbf{t})$: passing both captions and Gaussian noise images to BLIP as shown in Figure 2.

Visualization of α-tuning. Finally, we observe that α-tuning can consistently improve the performance. For visualization, we attach the results of α-tuning in Table 2. We show side-by-side frequency charts of $P_{train}(\mathbf{t})$ for positive and negative captions.

5 Additional Experimental Results

In this section, we apply our OTS generative approaches to more benchmarks, including two compositionality benchmarks Winoground (Thrush et al., 2022) and EqBen (Wang et al., 2023), and two classic large-scale retrieval benchmarks COCO (Lin et al., 2014) and Flickr30K (Young et al., 2014). While naively applying VisualGPTScore leads to bad performance on these benchmarks, our training-free debiasing solution can consistently improve its performance with a held-out validation set. Furthermore, we derive the optimal text-to-image (T-to-I) retrieval objective and show that OTS generative scores can achieve robust T-to-I performance without debiasing.

Evaluation protocols of Thrush et al. (2022). While prior analysis (Diwan et al., 2022; Yuksekgonul et al., 2022) suggests that Winoground is too out-of-distribution to evaluate compositionality, we argue that evaluation protocols of Winoground and EqBen are more robust for future evaluations of VLMs. In these two benchmarks, each sample consists of two image-text pairs, ensuring **uniform image and text priors**. For simplicity, we consider a single Winoground sample: $(\mathbf{i}_0, \mathbf{t}_0)$ and $(\mathbf{i}_1, \mathbf{t}_1)$. The joint probabilities are $P_{test}(\mathbf{i}_0, \mathbf{t}_0) = P_{test}(\mathbf{i}_1, \mathbf{t}_1) = 0.5$. Meanwhile, $P_{test}(\mathbf{i}_0, \mathbf{t}_1) = P_{test}(\mathbf{i}_1, \mathbf{t}_0) = 0$. Applying the law of total probability gives $P_{test}(t_0) = P_{test}(t_1) = 0.5$. A similar derivation can show that image priors are uniform too. In addition, Winoground's evaluation metrics (text score and image score) penalize unimodal shortcut solutions. For example, in I-to-T retrieval, the *text score* gets 1 point only if *both images* are matched to the correct caption. Therefore, "blind" solutions that choose the same text regardless of images will get 0 text score. Similarly, for T-to-I retrieval, the *image score* gets 1 point only if *both captions* are matched to the correct image.

Tuning α through cross validation. In Table 3-a, we first show that OTS generative scores without debiasing (α=0) lead to inferior performance on these I-to-T benchmarks. This confirms the importance of α-tuning; even a simple $\alpha = 1$ can consistently and often significantly improve their I-to-T results. Furthermore, we try to use a held-out validation set to tune for optimal $\alpha \in [0, 1]$. We sample half of the data as validation set to search for α^*_{val} (using a step size of 0.001) and report the performance on the other half. We repeat this process 10 times to and report the mean and std. We observe that the optimal alpha is usually stable under the same dataset, regardless of the sampled val set. For COCO and Flickr30K, we perform α-tuning using Recall@1 (R@1) on the official validation split. Because sampling additional Gaussian noise images can be too costly on these large-scale benchmarks, we directly approximate $P_{train}(\mathbf{t})$ by averaging the scores of testset images, without incurring any computational cost. More ablation studies such as α-tuning using testset can be found in Appendix B. We also include the results of the ITMScore of BLIP for reference. While our debiasing solution can always boost performance, we observe that generative approaches still lag behind the ITMScore. This motivates us to study biases of generative scores towards more "common" texts in Appendix C.

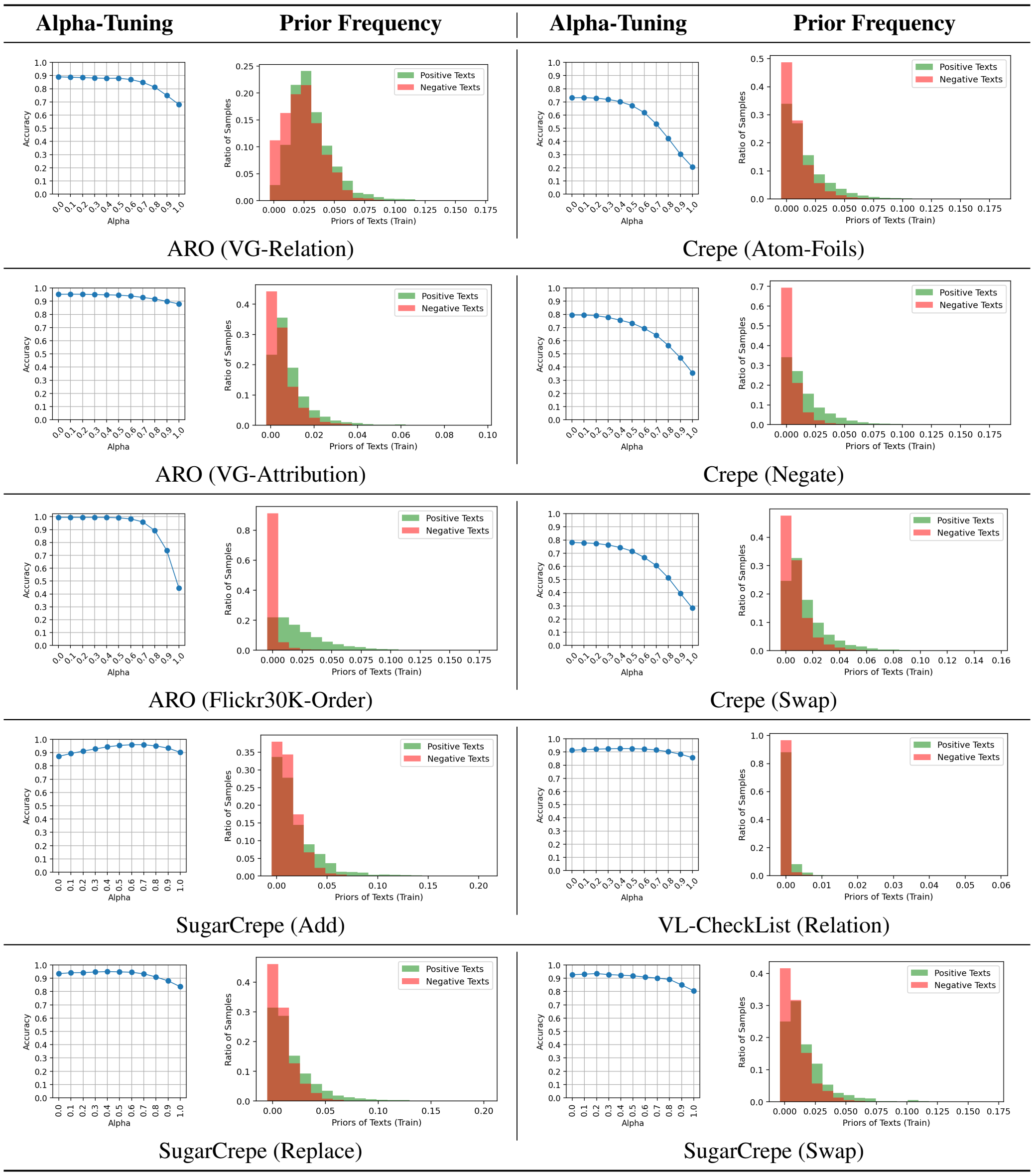

ARO (VG-Relation)

Crepe (Atom-Foils)

ARO (VG-Attribution)

Crepe (Negate)

ARO (Flickr30K-Order)

Crepe (Swap)

SugarCrepe (Add)

VL-CheckList (Relation)

SugarCrepe (Replace)

SugarCrepe (Swap)

Table 2: **α-tuning on I-to-T benchmarks and $P_{train}(\mathbf{t})$ frequency charts of both positive and negative captions.** Increasing α from 0 to 1 hurts performance on benchmarks with non-sensical negative captions such as ARO and Crepe. Such negative captions are easier to identify because of their low score under the language prior $P_{train}(\mathbf{t})$, implying such benchmarks may even be solved with blind algorithms that avoid looking at images. On the other hand, for benchmarks like SugarCrepe with more balanced $P_{train}(\mathbf{t})$ between positives and negatives, tuning α may lead to performance gain.

Extending to T-to-I retrieval. Though not the focus of our work, we also show that image-conditioned language models can be applied to T-to-I retrieval. Given a text caption $\mathbf{t}$, we can rewrite the Bayes optimal T-to-I retrieval objective as:

$$P_{test}(\mathbf{i}|\mathbf{t}) \propto P_{train}(\mathbf{t}|\mathbf{i}) * P_{train}(\mathbf{i}) \tag{10}$$

Equation 10 is hard to implement because we do not have access to $P_{train}(\mathbf{i})$. However, when $P_{train}(\mathbf{i})$ is approximately uniform, one can directly apply $P_{train}(\mathbf{t}|\mathbf{i})$ for optimal performance. We report T-to-I performance on all four benchmarks in Table 3-b, where our generative approach obtain competitive results compared against ITMScore, presumably because T-to-I retrieval is less affected by language biases.

Metric	Benchmark	ITMScore	$\frac{P_{train}(\mathbf{t}\vert\mathbf{i})}{P_{train}(\mathbf{t})^{\alpha}}$			
			α=0	α=1	α=α^*_{val}	α^*_{val}
Text Score	Winoground	$35.5_{(2.4)}$	$27.5_{(2.3)}$	$33.7_{(2.4)}$	$36.6_{(2.6)}$	$0.855_{(0.023)}$
	EqBen	$26.1_{(0.3)}$	$9.6_{(0.2)}$	$19.8_{(0.3)}$	$19.8_{(0.3)}$	$0.992_{(0.007)}$
R@1 / R@5	COCO	71.9 / 90.6	19.7 / 40.6	46.2 / 73.1	48.0 / 74.2	0.819
	Flickr30k	88.8 / 98.2	34.6 / 59.0	58.7 / 88.0	63.6 / 89.2	0.719

(a) α-tuning on val sets for I-to-T retrieval

Metric	Benchmark	ITMScore	$P_{train}(\mathbf{t}\vert\mathbf{i})$
Image Score	Winoground	15.8	21.5
	EqBen	20.3	26.1
R@1 / R@5	COCO	54.8 / 79.0	55.6 / 79.2
	Flickr30k	77.8 / 93.9	76.8 / 93.4

(b) T-to-I retrieval

Table 3: **Additional results on Winoground/EqBen/COCO/Flickr30K retrieval benchmarks.** Table (a) shows that tuning α can be essential for these compositionality and large-scale retrieval benchmarks. While OTS generative scores do not work well, debiasing with a larger α can consistently and often significantly improve I-to-T results on these tasks. To highlight the performance improvement, we mark results without debiasing ($\alpha = 0$) (in yellow) , debiasing with a fixed $\alpha = 1$ (in pink) , and cross-validation using held-out val sets ($\alpha = \alpha^*_{val}$) (in green) . Table (b) shows that OTS generative scores can obtain favorable results on classic T-to-I retrieval tasks, competitive with the ITMScore.

6 Discussion and Limitations

Summary. Our study shows the efficacy of *generative* pre-training scores in solving *discriminative* tasks. With the rise of generative pre-training in recent models like GPT-4 (OpenAI, 2023), we see our work as a reliable starting point for future tasks. We present a first-principles analysis to account for mismatching distributions over text between train and test data. Based on this, we introduce a robust training-free (zero-shot) solution to debias linguistic priors in generative scores, achieving consistent and often significant improvement on all I-to-T retrieval tasks. Our thorough analysis also explains the performance discrepancy of generative scores on different benchmarks, and we hope it can encourage future work to revisit the issue of language biases in vision-language benchmarks.

Limitations and future work. Our approach depends on generative VLMs pre-trained on noisy web datasets, which may result in inherited biases (Mehrabi et al., 2021). We do not explore fine-tuning techniques due to computational constraints, but it is possible to improve the I-to-T retrieval performance using hard negative samples, such as with controllable generation (Keskar et al., 2019). Furthermore, our analysis is based on simplified assumptions. For instance, the image-conditioned language model might not accurately represent $P_{train}(\mathbf{t}|\mathbf{i})$, a phenomenon we examine in Appendix C. Estimating $P_{train}(\mathbf{t})$ by sampling Gaussian noise images can be suboptimal; future VLMs could directly model $P_{train}(\mathbf{t})$, or use techniques like coreset selection (Guo et al., 2022) or dataset distillation (Wu et al., 2023) to sample more representative images. Finally, we leave debiasing on the T-to-I retrieval task for future work.

References

Harsh Agrawal, Karan Desai, Yufei Wang, Xinlei Chen, Rishabh Jain, Mark Johnson, Dhruv Batra, Devi Parikh, Stefan Lee, and Peter Anderson. Nocaps: Novel object captioning at scale. In *Proceedings of the IEEE/CVF international conference on computer vision*, pp. 8948–8957, 2019.

Jean-Baptiste Alayrac, Jeff Donahue, Pauline Luc, Antoine Miech, Iain Barr, Yana Hasson, Karel Lenc, Arthur Mensch, Katherine Millican, Malcolm Reynolds, et al. Flamingo: a visual language model for few-shot learning. *Advances in Neural Information Processing Systems*, 35:23716–23736, 2022.

Stanislaw Antol, Aishwarya Agrawal, Jiasen Lu, Margaret Mitchell, Dhruv Batra, C Lawrence Zitnick, and Devi Parikh. Vqa: Visual question answering. In *Proceedings of the IEEE international conference on computer vision*, pp. 2425–2433, 2015.

Yoshua Bengio, Réjean Ducharme, Pascal Vincent, and Christian Jauvin. A neural probabilistic language model. *Journal of Machine Learning Research*, 3:1137–1155, 2003.

Lorenzo Bertolini, Julie Weeds, and David Weir. Testing large language models on compositionality and inference with phrase-level adjective-noun entailment. In *Proceedings of the 29th International Conference on Computational Linguistics*, pp. 4084–4100, 2022.

Wieland Brendel and Matthias Bethge. Approximating cnns with bag-of-local-features models works surprisingly well on imagenet. *arXiv preprint arXiv:1904.00760*, 2019.

Tom Brown, Benjamin Mann, Nick Ryder, Melanie Subbiah, Jared D Kaplan, Prafulla Dhariwal, Arvind Neelakantan, Pranav Shyam, Girish Sastry, Amanda Askell, et al. Language models are few-shot learners. *Advances in neural information processing systems*, 33:1877–1901, 2020.

Paola Cascante-Bonilla, Khaled Shehada, James Seale Smith, Sivan Doveh, Donghyun Kim, Rameswar Panda, Gül Varol, Aude Oliva, Vicente Ordonez, Rogerio Feris, et al. Going beyond nouns with vision & language models using synthetic data. *arXiv preprint arXiv:2303.17590*, 2023.

Hyung Won Chung, Le Hou, S. Longpre, Barret Zoph, Yi Tay, William Fedus, Eric Li, Xuezhi Wang, Mostafa Dehghani, Siddhartha Brahma, Albert Webson, Shixiang Shane Gu, Zhuyun Dai, Mirac Suzgun, Xinyun Chen, Aakanksha Chowdhery, Dasha Valter, Sharan Narang, Gaurav Mishra, Adams Wei Yu, Vincent Zhao, Yanping Huang, Andrew M. Dai, Hongkun Yu, Slav Petrov, Ed Huai hsin Chi, Jeff Dean, Jacob Devlin, Adam Roberts, Denny Zhou, Quoc V. Le, and Jason Wei. Scaling instruction-finetuned language models. *ArXiv*, abs/2210.11416, 2022.

Béatrice Daille. *Approche mixte pour l'extraction automatique de terminologie: statistiques lexicales et filtres linguistiques*. PhD thesis, Ph. D. thesis, Université Paris 7, 1994.

Jia Deng, Wei Dong, Richard Socher, Li-Jia Li, Kai Li, and Li Fei-Fei. Imagenet: A large-scale hierarchical image database. In *2009 IEEE conference on computer vision and pattern recognition*, pp. 248–255. Ieee, 2009.

Jacob Devlin, Ming-Wei Chang, Kenton Lee, and Kristina Toutanova. Bert: Pre-training of deep bidirectional transformers for language understanding. *arXiv preprint arXiv:1810.04805*, 2018.

Anuj Diwan, Layne Berry, Eunsol Choi, David Harwath, and Kyle Mahowald. Why is winoground hard? investigating failures in visuolinguistic compositionality. *arXiv preprint arXiv:2211.00768*, 2022.

Sivan Doveh, Assaf Arbelle, Sivan Harary, Rameswar Panda, Roei Herzig, Eli Schwartz, Donghyun Kim, Raja Giryes, Rogerio Feris, Shimon Ullman, et al. Teaching structured vision&language concepts to vision&language models. *arXiv preprint arXiv:2211.11733*, 2022.

Sivan Doveh, Assaf Arbelle, Sivan Harary, Amit Alfassy, Roei Herzig, Donghyun Kim, Raja Giryes, Rogerio Feris, Rameswar Panda, Shimon Ullman, et al. Dense and aligned captions (dac) promote compositional reasoning in vl models. *arXiv preprint arXiv:2305.19595*, 2023.

Yuxin Fang, Wen Wang, Binhui Xie, Quan Sun, Ledell Wu, Xinggang Wang, Tiejun Huang, Xinlong Wang, and Yue Cao. Eva: Exploring the limits of masked visual representation learning at scale. *arXiv preprint arXiv:2211.07636*, 2022.

Jinlan Fu, See-Kiong Ng, Zhengbao Jiang, and Pengfei Liu. Gptscore: Evaluate as you desire. *arXiv preprint arXiv:2302.04166*, 2023.

Yash Goyal, Tejas Khot, Douglas Summers-Stay, Dhruv Batra, and Devi Parikh. Making the v in vqa matter: Elevating the role of image understanding in visual question answering. In *Proceedings of the IEEE conference on computer vision and pattern recognition*, pp. 6904–6913, 2017.

Chengcheng Guo, Bo Zhao, and Yanbing Bai. Deepcore: A comprehensive library for coreset selection in deep learning. In *Database and Expert Systems Applications: 33rd International Conference, DEXA 2022, Vienna, Austria, August 22–24, 2022, Proceedings, Part I*, pp. 181–195. Springer, 2022.

Christian Andreas Henning and Ralph Ewerth. Estimating the information gap between textual and visual representations. In *Proceedings of the 2017 ACM on International Conference on Multimedia Retrieval*, pp. 14–22, 2017.

Roei Herzig, Alon Mendelson, Leonid Karlinsky, Assaf Arbelle, Rogerio Feris, Trevor Darrell, and Amir Globerson. Incorporating structured representations into pretrained vision & language models using scene graphs. *arXiv preprint arXiv:2305.06343*, 2023.

Jack Hessel and Alexandra Schofield. How effective is bert without word ordering? implications for language understanding and data privacy. In *Proceedings of the 59th Annual Meeting of the Association for Computational Linguistics and the 11th International Joint Conference on Natural Language Processing (Volume 2: Short Papers)*, pp. 204–211, 2021.

Cheng-Yu Hsieh, Jieyu Zhang, Zixian Ma, Aniruddha Kembhavi, and Ranjay Krishna. Sugarcrepe: Fixing hackable benchmarks for vision-language compositionality. *arXiv preprint arXiv:2306.14610*, 2023.

Yufeng Huang, Jiji Tang, Zhuo Chen, Rongsheng Zhang, Xinfeng Zhang, Weijie Chen, Zeng Zhao, Tangjie Lv, Zhipeng Hu, and Wen Zhang. Structure-clip: Enhance multi-modal language representations with structure knowledge. *arXiv preprint arXiv:2305.06152*, 2023.

Chao Jia, Yinfei Yang, Ye Xia, Yi-Ting Chen, Zarana Parekh, Hieu Pham, Quoc Le, Yun-Hsuan Sung, Zhen Li, and Tom Duerig. Scaling up visual and vision-language representation learning with noisy text supervision. In *International Conference on Machine Learning*, pp. 4904–4916. PMLR, 2021.

Amita Kamath, Jack Hessel, and Kai-Wei Chang. Text encoders are performance bottlenecks in contrastive vision-language models. *arXiv preprint arXiv:2305.14897*, 2023.

Bingyi Kang, Saining Xie, Marcus Rohrbach, Zhicheng Yan, Albert Gordo, Jiashi Feng, and Yannis Kalantidis. Decoupling representation and classifier for long-tailed recognition. *arXiv preprint arXiv:1910.09217*, 2019.

Nitish Shirish Keskar, Bryan McCann, Lav R Varshney, Caiming Xiong, and Richard Socher. Ctrl: A conditional transformer language model for controllable generation. *arXiv preprint arXiv:1909.05858*, 2019.

Jiwei Li and Dan Jurafsky. Mutual information and diverse decoding improve neural machine translation, 2016.

Jiwei Li, Michel Galley, Chris Brockett, Jianfeng Gao, and Bill Dolan. A diversity-promoting objective function for neural conversation models. In *Proceedings of the 2016 Conference of the North American Chapter of the Association for Computational Linguistics: Human Language Technologies*, pp. 110–119, San Diego, California, June 2016. Association for Computational Linguistics. doi: 10.18653/v1/N16-1014. URL `https://aclanthology.org/N16-1014`.

Junnan Li, Ramprasaath Selvaraju, Akhilesh Gotmare, Shafiq Joty, Caiming Xiong, and Steven Chu Hong Hoi. Align before fuse: Vision and language representation learning with momentum distillation. *Advances in neural information processing systems*, 34:9694–9705, 2021.

Junnan Li, Dongxu Li, Caiming Xiong, and Steven Hoi. Blip: Bootstrapping language-image pretraining for unified vision-language understanding and generation. In *International Conference on Machine Learning*, pp. 12888–12900. PMLR, 2022.

Junnan Li, Dongxu Li, Silvio Savarese, and Steven Hoi. Blip-2: Bootstrapping language-image pretraining with frozen image encoders and large language models. *arXiv preprint arXiv:2301.12597*, 2023.

Tsung-Yi Lin, Michael Maire, Serge Belongie, James Hays, Pietro Perona, Deva Ramanan, Piotr Dollár, and C Lawrence Zitnick. Microsoft coco: Common objects in context. In *Computer Vision–ECCV 2014: 13th European Conference, Zurich, Switzerland, September 6-12, 2014, Proceedings, Part V 13*, pp. 740–755. Springer, 2014.

Zhiqiu Lin, Samuel Yu, Zhiyi Kuang, Deepak Pathak, and Deva Ramana. Multimodality helps unimodality: Cross-modal few-shot learning with multimodal models. *arXiv preprint arXiv:2301.06267*, 2023.

Yinhan Liu, Myle Ott, Naman Goyal, Jingfei Du, Mandar Joshi, Danqi Chen, Omer Levy, Mike Lewis, Luke Zettlemoyer, and Veselin Stoyanov. Roberta: A robustly optimized bert pretraining approach. *arXiv preprint arXiv:1907.11692*, 2019.

Zixian Ma, Jerry Hong, Mustafa Omer Gul, Mona Gandhi, Irena Gao, and Ranjay Krishna. Crepe: Can vision-language foundation models reason compositionally? *arXiv preprint arXiv:2212.07796*, 2022.

Ninareh Mehrabi, Fred Morstatter, Nripsuta Saxena, Kristina Lerman, and Aram Galstyan. A survey on bias and fairness in machine learning. *ACM Computing Surveys (CSUR)*, 54(6):1–35, 2021.

OpenAI. Gpt-4 technical report. *arXiv preprint arXiv:2303.08774*, 2023.

Isabel Papadimitriou, Richard Futrell, and Kyle Mahowald. When classifying grammatical role, bert doesn't care about word order... except when it matters. *arXiv preprint arXiv:2203.06204*, 2022.

Alec Radford, Jeffrey Wu, Rewon Child, David Luan, Dario Amodei, Ilya Sutskever, et al. Language models are unsupervised multitask learners. 2019.

Alec Radford, Jong Wook Kim, Chris Hallacy, Aditya Ramesh, Gabriel Goh, Sandhini Agarwal, Girish Sastry, Amanda Askell, Pamela Mishkin, Jack Clark, et al. Learning transferable visual models from natural language supervision. In *International conference on machine learning*, pp. 8748–8763. PMLR, 2021.

François Role and Mohamed Nadif. Handling the impact of low frequency events on co-occurrence based measures of word similarity. In *Proceedings of the international conference on Knowledge Discovery and Information Retrieval (KDIR-2011). Scitepress*, pp. 218–223, 2011.

Christoph Schuhmann, Richard Vencu, Romain Beaumont, Robert Kaczmarczyk, Clayton Mullis, Aarush Katta, Theo Coombes, Jenia Jitsev, and Aran Komatsuzaki. Laion-400m: Open dataset of clip-filtered 400 million image-text pairs. *arXiv preprint arXiv:2111.02114*, 2021.

Christoph Schuhmann, Romain Beaumont, Richard Vencu, Cade Gordon, Ross Wightman, Mehdi Cherti, Theo Coombes, Aarush Katta, Clayton Mullis, Mitchell Wortsman, et al. Laion-5b: An open large-scale dataset for training next generation image-text models. *arXiv preprint arXiv:2210.08402*, 2022.

Alexander Shapiro. Monte carlo sampling methods. *Handbooks in operations research and management science*, 10:353–425, 2003.

Aman Shrivastava, Ramprasaath R Selvaraju, Nikhil Naik, and Vicente Ordonez. Clip-lite: information efficient visual representation learning from textual annotations. *arXiv preprint arXiv:2112.07133*, 2021.

Harman Singh, Pengchuan Zhang, Qifan Wang, Mengjiao Wang, Wenhan Xiong, Jingfei Du, and Yu Chen. Coarse-to-fine contrastive learning in image-text-graph space for improved vision-language compositionality. *arXiv preprint arXiv:2305.13812*, 2023.

Koustuv Sinha, Robin Jia, Dieuwke Hupkes, Joelle Pineau, Adina Williams, and Douwe Kiela. Masked language modeling and the distributional hypothesis: Order word matters pre-training for little. *arXiv preprint arXiv:2104.06644*, 2021.

Ajinkya Tejankar, Maziar Sanjabi, Bichen Wu, Saining Xie, Madian Khabsa, Hamed Pirsiavash, and Hamed Firooz. A fistful of words: Learning transferable visual models from bag-of-words supervision. *arXiv preprint arXiv:2112.13884*, 2021.

Tristan Thrush, Ryan Jiang, Max Bartolo, Amanpreet Singh, Adina Williams, Douwe Kiela, and Candace Ross. Winoground: Probing vision and language models for visio-linguistic compositionality. In *Proceedings of the IEEE/CVF Conference on Computer Vision and Pattern Recognition*, pp. 5238–5248, 2022.

Tan Wang, Kevin Lin, Linjie Li, Chung-Ching Lin, Zhengyuan Yang, Hanwang Zhang, Zicheng Liu, and Lijuan Wang. Equivariant similarity for vision-language foundation models. *arXiv preprint arXiv:2303.14465*, 2023.

Zeyu Wang, Berthy Feng, Karthik Narasimhan, and Olga Russakovsky. Towards unique and informative captioning of images. In *European Conference on Computer Vision (ECCV)*, 2020.

Mitchell Wortsman, Gabriel Ilharco, Jong Wook Kim, Mike Li, Simon Kornblith, Rebecca Roelofs, Raphael Gontijo Lopes, Hannaneh Hajishirzi, Ali Farhadi, Hongseok Namkoong, et al. Robust fine-tuning of zero-shot models. In *Proceedings of the IEEE/CVF Conference on Computer Vision and Pattern Recognition*, pp. 7959–7971, 2022.

Xindi Wu, Zhiwei Deng, and Olga Russakovsky. Multimodal dataset distillation for image-text retrieval. *arXiv preprint arXiv:2308.07545*, 2023.

Ting Yao, Tao Mei, and Chong-Wah Ngo. Co-reranking by mutual reinforcement for image search. In *Proceedings of the ACM international conference on image and video retrieval*, pp. 34–41, 2010.

Peter Young, Alice Lai, Micah Hodosh, and Julia Hockenmaier. From image descriptions to visual denotations: New similarity metrics for semantic inference over event descriptions. *Transactions of the Association for Computational Linguistics*, 2:67–78, 2014.

Jiahui Yu, Zirui Wang, Vijay Vasudevan, Legg Yeung, Mojtaba Seyedhosseini, and Yonghui Wu. Coca: Contrastive captioners are image-text foundation models. *arXiv preprint arXiv:2205.01917*, 2022.

Weizhe Yuan, Graham Neubig, and Pengfei Liu. Bartscore: Evaluating generated text as text generation. In M. Ranzato, A. Beygelzimer, Y. Dauphin, P.S. Liang, and J. Wortman Vaughan (eds.), *Advances in Neural Information Processing Systems*, volume 34, pp. 27263–27277. Curran Associates, Inc., 2021. URL `https://proceedings.neurips.cc/paper/2021/file/e4d2b6e6fdeca3e60e0f1a62fee3d9dd-Paper.pdf`.

Mert Yuksekgonul, Federico Bianchi, Pratyusha Kalluri, Dan Jurafsky, and James Zou. When and why vision-language models behave like bag-of-words models, and what to do about it? *arXiv preprint arXiv:2210.01936*, 2022.

Susan Zhang, Stephen Roller, Naman Goyal, Mikel Artetxe, Moya Chen, Shuohui Chen, Christopher Dewan, Mona Diab, Xian Li, Xi Victoria Lin, et al. Opt: Open pre-trained transformer language models. *arXiv preprint arXiv:2205.01068*, 2022.

Tiancheng Zhao, Tianqi Zhang, Mingwei Zhu, Haozhan Shen, Kyusong Lee, Xiaopeng Lu, and Jianwei Yin. Vl-checklist: Evaluating pre-trained vision-language models with objects, attributes and relations. *arXiv preprint arXiv:2207.00221*, 2022.

Tony Zhao, Eric Wallace, Shi Feng, Dan Klein, and Sameer Singh. Calibrate before use: Improving few-shot performance of language models. In *International Conference on Machine Learning*, 2021.

APPENDIX

A COMPARISON TO PMI^k

By assuming $P_{test}(\mathbf{t})$ to be a “flatten” version of $P_{train}(\mathbf{t})$, our Equation 7 can interpolate between scenario 1 (same train and test priors) and 2 (balanced test priors):

$$P_{test}(\mathbf{t}) \propto P_{train}(\mathbf{t})^{1-\alpha} \quad \Rightarrow \text{Optimal score is } \frac{P_{train}(\mathbf{t}|\mathbf{i})}{P_{train}(\mathbf{t})^{\alpha}} \tag{11}$$

In fact, the above equation can be rewritten using the language of PMI^k (Role & Nadif, 2011; Daille, 1994), a well-known variant of PMI that controls the amount of debiasing (Li et al., 2016; Li & Jurafsky, 2016; Wang et al., 2020) in information retrieval:

$$\begin{align}
\frac{P_{train}(\mathbf{t}|\mathbf{i})}{P_{train}(\mathbf{t})^{\alpha}} &= \frac{P_{train}(\mathbf{t},\mathbf{i})}{P_{train}(\mathbf{i})P_{train}(\mathbf{t})^{\alpha}} \tag{12}\\
&\propto \frac{P_{train}(\mathbf{t},\mathbf{i})^{\frac{1}{\alpha}}}{P_{train}(\mathbf{i})P_{train}(\mathbf{t})} \quad \text{, as } P_{train}(\mathbf{i}) \text{ is constant in I-to-T} \tag{13}\\
&= \text{pmi}^{k}_{P_{train}}(\mathbf{t},\mathbf{i}), \text{ where } k = \frac{1}{\alpha} \geq 1 \tag{14}
\end{align}$$

where

$$\text{pmi}_{P}(\mathbf{t},\mathbf{i}) = \frac{P(\mathbf{t},\mathbf{i})}{P(\mathbf{t})P(\mathbf{i})} = \frac{P(\mathbf{t}|\mathbf{i})}{P(\mathbf{t})} = \frac{P(\mathbf{i}|\mathbf{t})}{P(\mathbf{i})} \tag{15}$$

PMI is an information-theoretic measure that quantifies the *association* between two variables (Yao et al., 2010; Henning & Ewerth, 2017; Shrivastava et al., 2021). In the context of image-text retrieval, it measures how much more (or less) likely the image-text pair co-occurs than if the two were independent. Eq. 15 has found applications in diverse sequence-to-sequence modelling tasks (Wang et al., 2020; Li & Jurafsky, 2016; Li et al., 2016) as a retrieval (reranking) objective. Compared to the conditional likelihood $P(\mathbf{t}|\mathbf{i})$, PMI reduces the learned bias for preferring ”common” texts with high marginal probabilities $P(\mathbf{t})$ (Li et al., 2016; Li & Jurafsky, 2016; Wang et al., 2020). This can be an alternative explanation for the effectiveness of our debiasing solutions.

B ABLATION STUDIES ON α-TUNING

Estimating $P_{train}(\mathbf{t})$ via null (Gaussian noise) images is more sample-efficient. We use Winoground to show that sampling Gaussian noise images to calculate $P_{train}(\mathbf{t})$ can be more efficient than sampling trainset images. As demonstrated in Table 4, a limited number of Gaussian noise images (e.g., 3 or 10) can surpass the results obtained with 1000 LAION images. Moreover, using null images produces less variance in the results.

Sample Size	Guassian Noise Images		Trainset Images	
	α=α^*_{test}	α^*_{test}	α=α^*_{test}	α^*_{test}
3	$35.95_{(0.5)}$	$0.821_{(0.012)}$	$32.20_{(1.6)}$	$0.706_{(0.150)}$
10	$36.25_{(0.4)}$	$0.827_{(0.016)}$	$33.60_{(0.9)}$	$0.910_{(0.104)}$
100	$36.35_{(0.1)}$	$0.840_{(0.010)}$	$34.70_{(0.6)}$	$0.910_{(0.039)}$
1000	$36.25_{(0.0)}$	$0.850_{(0.000)}$	$35.15_{(0.3)}$	$0.960_{(0.033)}$

Table 4: **Comparing sampling of Gaussian noise images and trainset images for estimating $P_{train}(\mathbf{t})$.** We report text scores of α-tuning on Winoground I-to-T retrieval task. We ablate 3/10/100/1000 Gaussian noise and LAION samples and report both mean and std using 5 sampling seeds. The optimal $\alpha^* \in [0, 1]$ is searched on testset via a step size of 0.001. The Gaussian noise images are sampled with a mean calculated from the LAION subset and a fixed std of 0.25.

Details of Gaussian noise samples. Unless otherwise specified, the Gaussian noise images are sampled with a mean of 1.0 and a standard deviation of 0.25. By default, we use 100 images for Winoground, 30 images for EqBen, and 3 images for the rest of the benchmarks. We also fix the sampling seed in our code to ensure reproducibility. We leave more advanced techniques of generating null images to future works.

Alternative approach on COCO/Flickr30k: estimating $P_{train}(\mathbf{t})$ using testset images. For large-scale retrieval benchmarks like COCO (Lin et al., 2014) and Flickr30k (Young et al., 2014), we can directly average scores of all candidate images (in the order of thousands) to efficiently approximate $P_{train}(\mathbf{t})$ without the need to sample additional images. This approach incurs zero computation cost as we have already pre-computed scores between each candidate image and text. We show in Table 5 that using testset images indeed results in better performance than sampling 3 Gaussian noise images.

Metric	Benchmark	$P_{train}(\mathbf{t}\vert\mathbf{i})$	Sampling Method	$\frac{P_{train}(\mathbf{t}\vert\mathbf{i})}{P_{train}(\mathbf{t})^{\alpha}}$		
				α=1	α=α^*_{val}	α^*_{val}
R@1 / R@5	COCO	19.7 / 40.6	Testset Images Null Images	46.2 / 73.1 24.4 / 52.6	48.0 / 74.2 40.4 / 66.6	0.819 0.600
	Flickr30k	34.6 / 59.0	Testset Images Null Images	58.7 / 88.0 27.8 / 62.2	63.6 / 89.2 48.5 / 79.0	0.719 0.427

Table 5: **I-to-T retrieval on COCO/Flickr30k using different sampling methods.** Estimating $P_{train}(\mathbf{t})$ by averaging the scores of testset images (with zero computational cost) demonstrates superior performance compared to sampling additional Gaussian noise images.

Tuning α with a validation set. In Table 6, similar performance trends are observed across validation and test splits of COCO and Flickr30k I-to-T retrieval benchmarks using the same $\alpha \in [0, 1]$. Furthermore, α^*_{test} and α^*_{val} are empirically close. As such, our method can function as a reliable training-free debiasing method. Future studies may explore fine-tuning methods to further improve the debiasing performance.

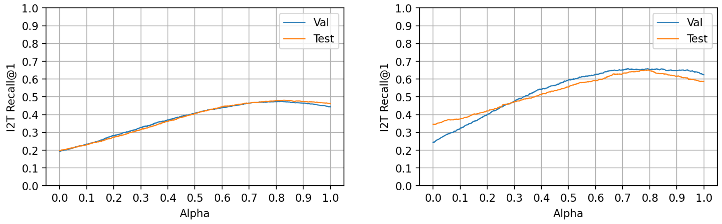

(b) Alpha-tuning on COCO Retrieval

(c) Alpha-tuning on Flickr Retrieval

Table 6: **α-tuning results on both val set and test set for COCO/Flickr30k I-to-T retrieval.** We observe that validation and test performance are strongly correlated while we interpolate $\alpha \in [0, 1]$.

C Is VisualGPTScore a Biased Estimator of $P_{train}(\mathbf{t}|\mathbf{i})$?

Retrieval performance on trainset (LAION). This paper is built on the assumption that VisualGPTScore is a reliable estimator of $P_{train}(\mathbf{t}|\mathbf{i})$. However, this simplifying assumption does not completely hold for the BLIP model we examine. We speculate that such OTS generative scores are biased towards more common texts. We witness this same phenomenon in Table 7, where we perform image-text retrieval on random subsets from training distribution LAION-114M (Li et al., 2022).

Modelling the language bias in VisualGPTScore. As evidenced in Table 7, we believe VisualGPTScore is biased towards more common texts due to modelling error. To consider this error in our analysis, we rewrite the VisualGPTScore as:

$$\textbf{VisualGPTScore}(\mathbf{t}, \mathbf{i}) := \hat{P}_{train}(\mathbf{t}|\mathbf{i}) = P_{train}(\mathbf{t}|\mathbf{i}) \cdot P_{train}(t)^{\beta}, \tag{16}$$

where $\hat{P}$ represents the (biased) model estimate and P represents the true distribution. The model bias towards common texts is encoded by an unknown parameter β.

Monte Carlo estimation using $\hat{P}$. Because our Monte Carlo sampling method relies on $\hat{P}_{train}(\mathbf{t}|\mathbf{i})$, it is also a biased estimator of $P_{train}(\mathbf{t})$:

Dataset Size	I-to-T Retrieval					T-to-I Retrieval	
	ITM	$\frac{P_{train}(\mathbf{t}\mid\mathbf{i})}{P_{train}(\mathbf{t})^{\alpha}}$				ITM	$P_{train}(\mathbf{t}\mid\mathbf{i})$
		α=0	α=1	α=α^*	α^*		
100	**96.0**	59.0	94.0	**95.0**	0.535	95.0	**97.0**
1000	**90.9**	37.1	71.7	85.7	0.733	92.0	**93.1**
2000	**87.2**	32.8	62.3	64.3	0.840	87.8	**89.8**
5000	**79.8**	25.1	50.9	54.1	0.727	81.9	**84.4**

(a) Performance on LAION trainset retrieval

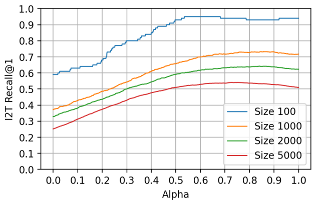

(b) Alpha-tuning on LAION

Table 7: **Retrieval performance on randomly sampled LAION114M subsets with varied sizes.** Table (a) shows that while OTS generative scores are robust for T-to-I retrieval, its performance degrades on I-to-T retrieval tasks when the number of candidate texts increases. This implies that OTS generative scores suffer from language biases towards certain texts even in the training set. Nonetheless, we show that our debiasing solution using either $\alpha = 1$ or optimal $\alpha^* \in [0, 1]$ with a step size of 0.001, can consistently boost the performance. Figure (b) visualizes α-tuning results on LAION subsets, where each curve represents a different sample size.

$$\hat{P}_{train}(\mathbf{t}) := \frac{1}{n}\sum_{k=1}^{n}\hat{P}_{train}(\mathbf{t}|\mathbf{i}_k) = P_{train}(\mathbf{t})^{1+\beta}. \tag{17}$$

Rewriting optimal I-to-T objective with $\hat{P}$. We can rewrite Equation 4 as:

$$P_{test}(\mathbf{t}|\mathbf{i}) \propto P_{train}(\mathbf{t}|\mathbf{i})\frac{P_{test}(\mathbf{t})}{P_{train}(\mathbf{t})} \tag{18}$$

$$= \hat{P}_{train}(\mathbf{t}|\mathbf{i})\frac{P_{test}(\mathbf{t})}{P_{train}(\mathbf{t})^{1+\beta}} \tag{19}$$

$$= \hat{P}_{train}(\mathbf{t}|\mathbf{i})\frac{P_{test}(\mathbf{t})}{\hat{P}_{train}(\mathbf{t})} \tag{20}$$

α-tuning with $\hat{P}$. Using Equation 20, we can reformulate α-tuning (Equation 7) as follows:

$$P_{test}(\mathbf{t}) \propto P_{train}(\mathbf{t})^{1-\hat{\alpha}} \quad \Rightarrow \text{Optimal score is } \frac{\hat{P}_{train}(\mathbf{t}|\mathbf{i})}{\hat{P}_{train}(\mathbf{t})^{\alpha}} \tag{21}$$

where $\alpha = \frac{\hat{\alpha}+\beta}{1+\beta}$. Notably, the above equation has the same structure as before (Equation 7). This implies that even if $P_{train}(\mathbf{t}) = P_{test}(\mathbf{t})$, we still anticipate $\alpha = \frac{\beta}{1+\beta} \neq 0$. This accounts for why the optimal α is not 0 when we perform I-to-T retrieval on trainset in Table 7.

Implication for vision-language modelling. Our analysis indicates that similar to generative LLMs (Li et al., 2016; Li & Jurafsky, 2016), contemporary image-conditioned language models also experience issues related to imbalanced learning (Kang et al., 2019). Potential solutions could be: (a) refined sampling techniques for Monte Carlo estimation of $P(\mathbf{t})$ such as through dataset distillation (Wu et al., 2023), and (b) less biased modelling of $P(\mathbf{t}|\mathbf{i})$ such as through controllable generation (Keskar et al., 2019).

D Experiments with BLIP-2

We provide BLIP-2 results for completeness.

BLIP-2 (Li et al., 2023) overview. BLIP-2 leverages frozen pre-trained image encoders (Fang et al., 2022) and large language models (Chung et al., 2022; Zhang et al., 2022) to bootstrap vision-language pre-training. It proposes a lightweight Querying Transformer (Q-Former) that is trained in two stages. Similar to BLIP (Li et al., 2022), Q-Former is a mixture-of-expert model that can calculate ITC, ITM, and captioning loss given an image-text pair. Additionally, it introduces a set of trainable query tokens, whose outputs serve as *visual soft prompts* prepended as inputs to LLMs. In its first training stage, Q-Former is fine-tuned on the same LAION dataset using the same objectives

(ITC+ITM+captioning) as BLIP. In the second stage, the output query tokens from Q-Former are fed into a frozen language model, such as FLAN-T5 (Chung et al., 2022) or OPT (Chung et al., 2022), after a linear projection trained only with captioning loss. BLIP-2 achieves state-of-the-art performance on various vision-language tasks with significantly fewer trainable parameters.

BLIP-2 results. We present retrieval performance of the BLIP-2 model that uses ViT-L as the frozen image encoder. We report results for both the first-stage model (denoted as Q-Former) and the second-stage model which employs FLAN-T5 (Chung et al., 2022) as the frozen LLM.

Benchmark	Dataset	Random	w. Q-Former			w. Flan-T5
			ITC	ITM	$P_{train}(\mathbf{t}\|\mathbf{i})$	$P_{train}(\mathbf{t}\|\mathbf{i})$
ARO	VG-Relation	50.0	46.4	67.2	90.7	89.1
	VG-Attribution	50.0	76.0	88.1	94.3	90.9
	COCO-Order	20.0	28.5	25.2	96.8	99.3
	Flickr30K-Order	20.0	25.3	28.6	97.5	99.7
Crepe	Atom-Foils	16.7	20.8	20.9	74.7	69.7
	Negate	16.7	13.4	14.2	79.1	90.0
	Swap	16.7	13.4	18.0	79.5	79.1
VL-CheckList	Object	50.0	89.7	89.2	90.1	84.1
VL-CheckList	Attribute	50.0	76.6	79.3	73.9	70.6
VL-CheckList	Relation	50.0	70.5	72.3	89.9	56.7
SugarCrepe	Replace	50.0	86.7	88.5	93.0	82.4
SugarCrepe	Swap	50.0	69.8	80.9	91.2	80.8
SugarCrepe	Add	50.0	86.5	88.0	92.7	76.2

Table 8: **BLIP-2 on ARO/Crepe/VL-CheckList/SugarCrepe.**

Benchmark	Model	I-To-T (Text Score)						T-To-I (Image Score)		
		ITC	ITM	$\frac{P_{train}(\mathbf{t}\|\mathbf{i})}{P_{train}(\mathbf{t})^{\alpha}}$				ITC	ITM	$P_{train}(\mathbf{t}\|\mathbf{i})$
				α=0	α=1	α=α^*	α^*			
Winoground	BLIP	28.0	35.8	27.0	33.0	36.5	0.836	9.0	15.8	21.5
	BLIP2-QFormer	30.0	42.5	24.3	29.3	33.0	0.882	10.5	19.0	20.0
	BLIP2-FlanT5	-	-	25.3	31.5	34.3	0.764	-	-	19.5
EqBen (Val)	BLIP	20.9	26.0	9.6	19.8	19.8	0.982	20.3	20.3	26.1
	BLIP2-QFormer	32.1	36.2	12.2	21.9	22.2	0.969	23.4	28.4	26.6
	BLIP2-FlanT5	-	-	8.5	22.0	22.0	1.000	-	-	20.9

Table 9: **BLIP-2 on Winoground/EqBen.**

E Additional Reports

Computational resources. All experiments use a single NVIDIA GeForce 3090s GPU.

Details of Table 1. For CLIP, LAION2B-CLIP, and LAION5B-CLIP, we report the results from Hsieh et al. (2023) using the ViT-B-32, ViT-bigG-14, and xlm-roberta-large-ViT-H-14 models respectively. The results of NegCLIP, Structure-CLIP, SVLC, SGVL, DAC-LLM, and DAC-SAM are directly copied from their original papers. We run BLIP-ITC and BLIP-ITM using our own codebase, which will be released to the public.

Group scores on Winoground/EqBen using BLIP (Table 10).

Method	Winoground			EqBen		
	Text Score	Image Score	Group Score	Text Score	Image Score	Group Score
ITCScore	28.0	9.0	6.5	20.9	20.3	10.6
ITMScore	35.8	15.8	13.3	26.0	20.3	12.6
VisualGPTScore$^{\alpha^*}$	36.5	21.5	16.8	20.4	26.1	11.7

Table 10: Performance comparison of BLIP's ITCScore, ITMScore, and α-tuned VisualGPTScore$^{\alpha^*}$ on Winoground (all) and EqBen (val).

Fine-grained tags on Winoground (Table 11).

Performance on SugarCrepe (Table 12).

Dataset	Size	Method	Text Score	Image Score	Group Score
NoTag	171	ITCScore	32.6	11.6	8.1
		ITMScore	41.9	21.5	19.2
		VisualGPTScore$^{\alpha^*}$	43.0	28.5	23.8
NonCompositional	30	ITCScore	43.3	16.7	16.7
		ITMScore	50.0	23.3	16.7
		VisualGPTScore$^{\alpha^*}$	43.3	33.3	26.7
AmbiguouslyCorrect	46	ITCScore	32.6	8.7	6.5
		ITMScore	28.3	6.5	2.2
		VisualGPTScore$^{\alpha^*}$	26.1	19.6	8.7
VisuallyDifficult	38	ITCScore	29.0	7.9	7.9
		ITMScore	26.3	10.5	7.9
		VisualGPTScore$^{\alpha^*}$	31.6	13.2	7.9
UnusualImage	56	ITCScore	32.5	8.9	8.9
		ITMScore	21.4	10.7	7.1
		VisualGPTScore$^{\alpha^*}$	30.4	10.7	8.9
UnusualText	50	ITCScore	20.0	8.0	6.0
		ITMScore	38.0	12.0	12.0
		VisualGPTScore$^{\alpha^*}$	30.0	18.0	12.0
ComplexReasoning	78	ITCScore	16.7	2.6	1.3
		ITMScore	21.8	5.1	2.6
		VisualGPTScore$^{\alpha^*}$	21.8	10.3	6.4

Table 11: BLIP performance on Winoground subtags (Diwan et al., 2022). We report the number of test instances for each subtag and their respective text score, image score, group score.

Method	Model	SugarCrepe			
		Replace	**Swap**	**Add**	**AVG**
Human Performance	-	98.67	99.50	99.00	99.06
Random Chance	-	50.00	50.00	50.00	50.00
Text-Only Baseline	Vera	49.46	49.30	49.50	49.42
	Grammar	50.00	50.00	50.00	50.00
$P_{LLM}(\mathbf{t})$	Bart	48.41	51.93	61.16	53.83
	Flan-T5	51.41	57.59	40.94	49.98
	OPT	58.53	66.58	45.78	56.96
$P_{train}(\mathbf{t})$	BLIP	75.90	77.14	70.89	74.64
ITCScore	CLIP-LAION2B	86.50	68.56	88.37	81.14
	CLIP-LAION5B	84.98	67.95	89.62	80.85
	BLIP	85.76	73.79	85.66	81.74
	BLIP-2	86.66	69.77	86.50	80.98
	NegCLIP-SugarCrepe	88.27	74.89	90.16	84.44
ITMScore	BLIP	88.68	81.29	87.57	85.85
	BLIP2-Qformer	88.45	80.87	87.96	85.76
$P_{train}(\mathbf{t}\|\mathbf{i})$	BLIP	**93.33**	**91.00**	**90.98**	**91.77**
	BLIP2-Qformer	**93.00**	**91.24**	**92.69**	**92.31**
	BLIP2-FlanT5	82.44	76.57	76.24	78.42
$\frac{P_{train}(\mathbf{t}\|\mathbf{i})}{P_{train}(\mathbf{t})^{\alpha^*}}$	BLIP	**95.09**	**92.39**	**97.36**	**94.95**
	BLIP2-Qformer	**94.62**	**92.27**	**97.58**	**94.82**
	BLIP2-FlanT5	85.69	78.80	91.76	85.42

Table 12: **Performance on SugarCrepe (Hsieh et al., 2023).** SugarCrepe is the most recent visio-linguistic compositionality benchmark which improves upon previous Crepe (Ma et al., 2022) by using state-of-the-art large language models (including ChatGPT), instead of rule-based templates, to generate more natural negative text captions. We show that text-only baselines and LLM-based methods indeed fail to succeed on SugarCrepe. However, our OTS generative approaches still achieve competitive results compared against SOTA discriminative approaches. The results of human performance, text-only baseline, and SOTA CLIP and NegCLIP-SugarCrepe are directly taken from the Hsieh et al. (2023). For other approaches, we evaluate their performance following the same procedure as described in main texts.

F Benchmark Visualization

We include random samples from each benchmark in Table 13.

Dataset	Image	Positive Caption	Negative Caption(s)
VG-Relation		the bus is to the right of the trees	the trees is to the right of the bus
VG-Attribution	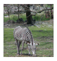	the striped zebra and the large tree	the large zebra and the striped tree
COCO-Order		two dogs sharing a frisby in their mouth in the snow	two frisby sharing a mouth in their snow in the dogs in dogs the in frisby sharing two mouth their a snow two dogs sharing in a frisby their mouth in snow the a frisby in the snow two dogs sharing their mouth in
Flickr30K-Order		a white duck spreads its wings while in the water	a white wings spreads its water while in the duck a white duck the its wings while in water spreads white a duck spreads its wings in while the water while in the spreads its wings water a white duck
SugarCrepe Add-Attribute		They are going to serve pizza for lunch today.	They are going to serve pizza topped with pineapple for lunch today.
SugarCrepe Add-Object		A man kisses the top of a woman's head.	A man kisses the top of a woman's head with a flower in his hand.
SugarCrepe Replace-Attribute		A kid standing with a small suitcase on a street.	A kid standing with a big suitcase on a street.
SugarCrepe Replace-Object	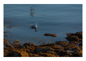	A duck floating in the water near a bunch of grass and rocks	A swan floating in the water near a bunch of grass and rocks.
SugarCrepe Replace-Relation		A clock tower stands in front of a large mirrored sky scraper.	A clock tower stands behind a large mirrored sky scraper.
SugarCrepe Swap-Attribute		A tennis player is taking a swing on a red court.	A red player is taking a swing on a tennis court.
SugarCrepe Swap-Object	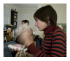	A woman holding a game controller with a man looking on.	A man holding a game controller with a woman looking on.
Crepe-AtomFoils		microwave in a kitchen, and sink in a kitchen.	microwave in a cupboard, and sink in a kitchen microwave in a bar, and sink in a kitchen line in a kitchen, and sink in a kitchen microwave in a kitchen, and shower in a kitchen microwave in a kitchen, and tap in a kitchen
Crepe-Negate		a chair next to a table, with the back of the chair visible.	A chair is not next to a table, with the back of the chair visible A chair next to a table, with the back not of the chair visible A chair next to a table, with the back of the chair visible A chair next to a table, with something of the chair visible. There is no back. There is no chair next to a table, with the back of the chair visible
Crepe-Swap		a car driving on a road with a line next to a tree.	a car driving on a bright green leaves with a line next to a tree a bright green leaves driving on a road with a line next to a tree a car driving on a tree with a line next to a road a car driving on a road with a line next to a white car a car driving on a road with a line next to a street
VL-CheckList Relation (spatial)		person read book	person carry book
VL-CheckList Relation (action)		sign near boy	sign far from book
Winoground		a person on top of the world	the world on top of a person
		the world on top of a person	a person on top of the world
EqBen	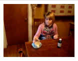	The person is touching the dish which is in front of him/her.	The person is holding the dish which is in front of him/her.
		The person is holding the dish which is in front of him/her.	The person is touching the dish which is in front of him/her.

Table 13: **Visualization of benchmarks.** ARO (VG-Relation/VG-Attribution/COCO-Order/Flickr30K-Order), Crepe (AtomFoils/Negate/Swap), VL-CheckList (Object/Attribute/Relation), SugarCrepe (Replace/Swap/Add) are constructed by generating hard negative captions for an image-text pair. On the other hand, each sample of Winoground and EqBen has two image-text pairs.